Progress In Electromagnetics Research M, Vol. 116, 1–10, 2023

A Polarization Reconfigurable Rectangular Dielectric Resonator Antenna Using PIN Diode for X-Band Applications

Akrem A. Soltan[1, *], Salam K. Khamas[1], and Salman M. Salman[2]

Abstract—A polarization reconfigurable dielectric resonator antenna (DRA) is proposed for X-band applications. The antenna provides circularly polarized (CP) or linearly polarized (LP) radiations at the same frequency band. Altering the states of two PIN diode switches offers a choice of one of three polarization options: (i) LP radiation; (ii) left-hand CP (LHCP) radiation; (iii) right-hand CP (RHCP) radiation. The simulations and measurements are in close agreement, indicating that the LHCP and RHCP radiations have reconfigurable polarization traits with a 21.3% impedance bandwidth ranging from 9.6 to 11.9 GHz and a 3.4% for the LP radiation that extends from 10.2 to 10.5 GHz. There is simultaneously a maximum gain of 6.9 dBic with a circa 4% axial ratio (AR) bandwidth for the LHCP and RHCP radiations.

1. INTRODUCTION

For high frequency applications, the dielectric resonator antenna appears most effective due to numerous advantages, including high radiation efficiency, no metallic and surface wave losses, flexible geometry, cost-effectiveness, low profile, and wide accessibility of various permittivity materials with dielectric constants range of 1–100 [1, 2]. Progress made in wireless communication systems has introduced increased performance demands on the antenna; therefore, a single device is expected to offer multi-functionality within a restricted space in order to satisfy the various application needs. As a result, reconfigurable antennas are frequently utilised since they are capable of switching between multiple states, hence they offer a variety of functions using a single antenna [3]. When a multi-standard wireless communication system needs to achieve polarization diversity, a popular choice is to employ polarization switchable antennas. Diverse polarization schemes can decrease multipath fading losses, which both improve the capacity of the system and minimise its size [4]. There are four types of reconfigurability strategies [5], electrical, mechanical, material, and optical. The PIN diodes can rapidly carry out the switching and manage comparatively high currents. One typical application is in microwave circuits. The potential for contact and inertial impacts means that outdated electromechanical RF switching elements are inherently poor response devices [6–8].

Various polarization reconfigurable antennas that utilise liquid to alter the polarization state have been proposed [9, 10]. For example, a 3D DRA container has been designed with left-hand and right-hand zones that are filled with ethyl acetate to achieve RHCP and LHCP waves [9]. In another study, polarization reconfigurability has been achieved through the injection of water into four cavities created in a cylindrical acrylic holder that operates as a DRA with different states, LHCP, RHCP, and LP [10]. However, due to their large dimensions, liquid DRAs function in static systems only. Additionally, any modification of the liquid properties can alter the operating frequency and CP bandwidth. Therefore, the liquid must be treated very carefully prior to injection into the DRAs for polarization reconfigurability.

Received 19 January 2023, Accepted 28 February 2023, Scheduled 11 March 2023

* Corresponding author: Akrem Amar Soltan (aasoltan1@sheffield.ac.uk).

[1] Department of Electrical Engineering and Electronics, University of Sheffield, Sheffield S1 4DT, UK. [2] Department of Biomedical Engineering, Al-Nahrain University, Baghdad, Iraq.

Furthermore, the pump used to inject the liquid increases the size and complexity of the system. On the other hand, numerous studies have utilised PIN diodes in the design of reconfigurable antennas. The primary benefits of PIN diode switches are operation speed and packaging simplicity. Generally, PIN diode switches have under 100 ns switching time. A key trait of a PIN diode is that it is composed of almost pure resistance at microwave frequencies. For the biasing, the range of resistance values could be between 1 Ω and 20,000 Ω. Additionally, a PIN diode switch provides improved controllability. A complex cylindrical DRA configuration has been proposed for the 5th generation (5G) band of 3.1–3.85 GHz with switchable polarizations by altering the states of the PIN diodes which is located under the DRA [11]. The achieved three polarization states are RHCP, LHCP, and LP with respective impedance bandwidths of 27.2%, 27.35%, and 21.6%. The antenna offers a gain of 5.5 dBi in the three polarization states.

An alternative multi-polarization DRA design has been proposed by etching a cross-slot in the ground plane to achieve circular polarization, where the dimensions of the cross-slot arms have been chosen to accommodate the PIN diodes that control the switching [12]. In all polarization states, the antenna sustained 20% (2.4–2.8 GHz) impedance bandwidth albeit with an extremely narrow AR bandwidth of 1%. Furthermore, a recent study has incorporated a PIN diode-based polarizer with a cylindrical DRA to accomplish polarization reconfigurability. The proposed antenna band (3.1–4.76 GHz) with respective impedance bandwidths of 3.42%, 14.56%, and 12.54% for the LP, RHCP, and LHCP radiations. The achieved AR bandwidths are 8.54% and 9.73% for the RHCP and LHCP radiations with a maximum gain of 5.67 dBi in all operating states [13]. The design that is being proposed ensures that different polarization states and multiband operation can be achieved by controlling the biasing state of switches such as RHCP, LHCP, and LP at 2.4-/5.8-GHz WLAN [14]. Additionally, the LP states have achieved frequency diversity at 2.6 GHz with a maximum gain of 4.6 dBi. A circularly polarized multiple-input multiple-output antenna array was proposed for C-band applications [15]. The antenna utilized two input and four output ports, which were controlled by four PIN diodes to switch between RHCP and LHCP. The antenna exhibited an impedance bandwidth and axial ratio bandwidths of 85.2% (4.48 to 8.21 GHz) and 46.3% (4.31–6.91), respectively, with a maximum gain of 9.8 dBic.

In this article, PIN diodes are utilised in the design of a reconfigurable rectangular DRA with polarization diversity for the X band applications. The slot-fed antenna offers a low profile, simple and effective feeding through a microstrip line feed, and a simple integrated biasing circuit to achieve three different polarisations. The antenna exhibits wide impedance bandwidths for the RHCP and LHCP radiations and a reasonable impedance bandwidth for the LP radiation. The simulations have been implemented using CST microwave studio with a close agreement between the simulated and measured results.

2. APPLICATION OF PIN DIODE

In RF and microwave front-end application systems, PIN diodes are the most frequently utilised switching devices. Figure 1 depicts the RF equivalent circuits of the MA4SPS402 PIN diode for the ON, forward bias, and OFF, reverse bias, states. Figure 1(a) presents the equivalent circuit of a forward-biased diode, which involves a resistor of $R_{\mathrm{ON}} = 5.2\,\Omega$ in series with an inductor of $L_S = 0.45$ nH. On the other hand, the equivalent circuit of a reverse biased diode is presented in Figure 1(b), which consists of a capacitor $C_{\mathrm{OFF}} = 0.045$ pF in parallel with a resistor of $R_{\mathrm{OFF}} = 20\,\mathrm{k}\Omega$ represents the diode's net

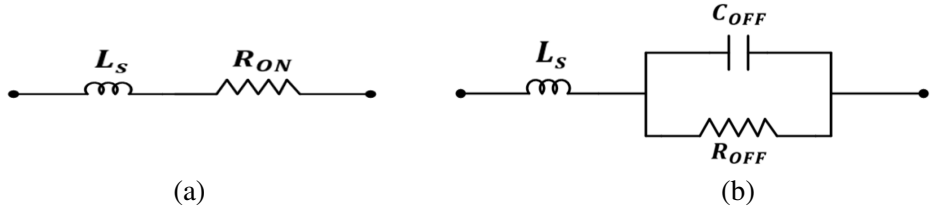

Figure 1. Equivalent circuits of a PIN diode; (a) Forward bias (ON) state, (b) reversed bias (OFF) state.

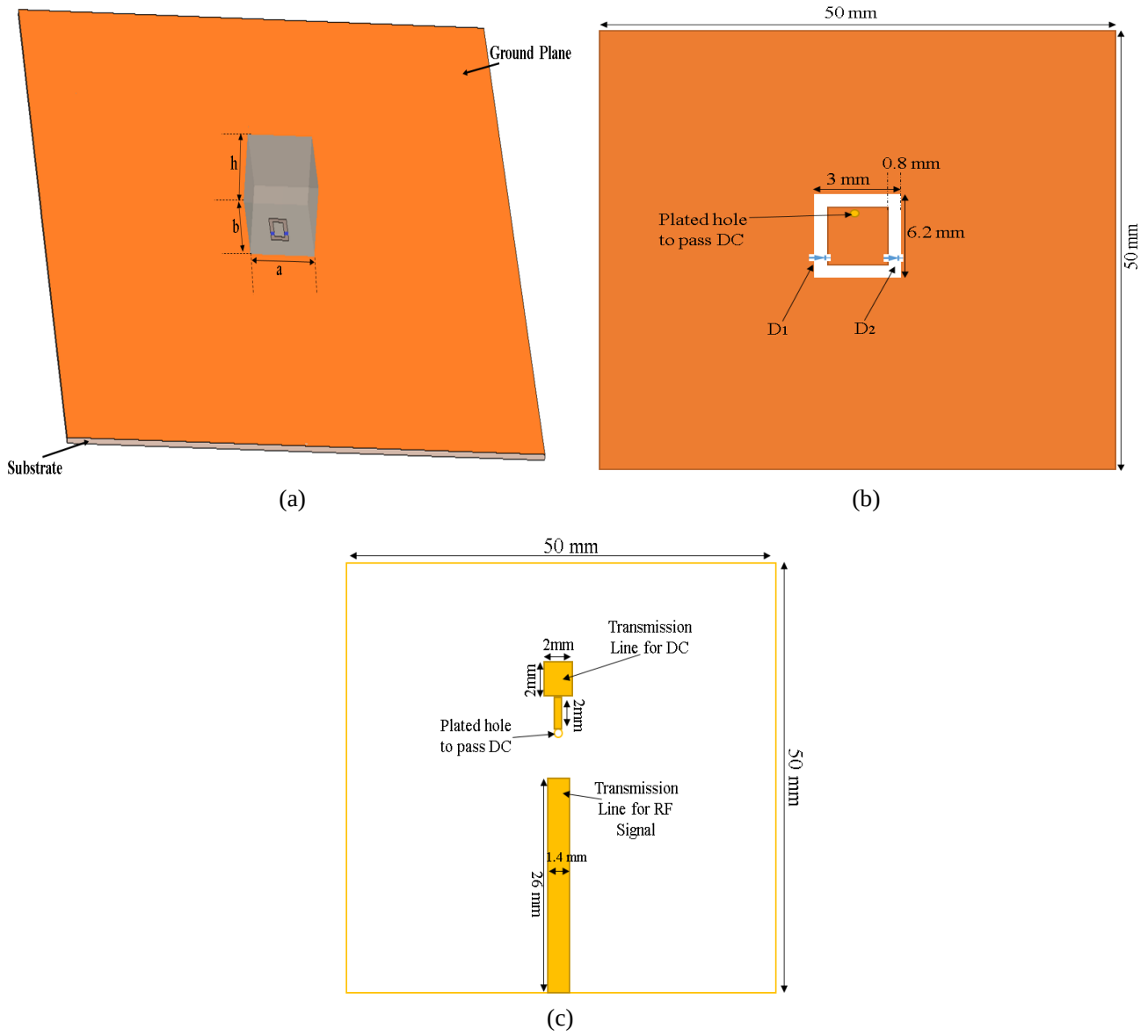

Figure 2. The geometry of the slot-fed reconfigurable RDRA, (a) proposed configuration, (b) top view, (c) bottom view.

dissipative resistance. The parallel RC circuit is connected in series with an inductor of $L_S = 0.45\,\text{nH}$. The equivalent circuit of a PIN diode is obtained from the datasheet [16]. The proposed configuration is presented in Figure 2, where it can be noted that the PIN diodes are located on two opposite sides of the feeding rectangular ring slot. In order to eliminate the need for separate bias lines, biasing has been achieved by dividing the ground plane into separate sections of opposite polarities as demonstrated in Figure 2(b). In addition, two RF choke inductors of 30 nH each, have been employed to stop RF currents from passing through the biasing wires and damaging the equipment and/or impacting the antenna performance.

3. ANTENNA DESIGN

The proposed polarization reconfigurable rectangular DRA, which has been designed using alumina with respective dielectric constant and loss tangent of $\epsilon_r = 9.9$ and loss tangent < 0.002. The selected

length, width, and height of $a = 10\,\text{mm}$, $b = 8.6\,\text{mm}$, and $h = 8.8\,\text{mm}$, which correspond to 0.36λ, 0.30λ, and 0.31λ, respectively, at 10.75 GHz that have been determined by following the procedure described in [17]. As illustrated in Figure 2(a), the DRA has been placed on top of a metal ground plane that is supported by a Rogers RO4350B substrate with respective size and thickness of 50 mm and 0.8 mm and has a dielectric constant and loss tangent of 3.48 and 0.0037, respectively. The ground plane and substrate have identical dimensions. A rectangular ring slot has been utilised to excite the DRA with dimensions of 6.2 mm × 3 mm and a slot width of 0.8 mm. It should be noted that CP can only be achieved when a short circuit section is created along the rectangular ring slot. The required polarisation sense can be achieved by creating the short circuit on the long left, or right hand, of the rectangular ring slot. However, the size and position of the short circuit need to be optimized in order to achieve the CP radiation. In this study, the short circuit has been created by using a forward-biased PIN diode to facilitate the polarisation reconfigurability. The dimensions of the used diode are predetermined from the data sheet, and the position has been optimised using CST.

The ground plane has been cut into two parts to control the PIN diode biasing as demonstrated in Figure 2(b). The bottom view of the substrate illustrates a microstrip transmission line for the RF signal, and the other line is to pass the DC signal to the inner smaller ground plane section through the plated hole as shown in Figure 2(c). Figure 3 illustrates the simulated reflection coefficients $|S_{11}|$ and AR for different switch positions; top, middle, and bottom of the long side of the feeding slot. Table 1 demonstrates that the best AR bandwidth has been achieved when the switch position is located at either the bottom or top of the long side of the rectangular ring slot. On the other hand, the widest impedance bandwidth has been achieved when the switch is placed at the bottom of the longest slot side. Although the top and bottom switch locations provide the same AR bandwidth, the impedance bandwidths are different since the position of the switch is different with respect to the feeding microstrip line, which is of less significance for the far-field characteristics. The difference in the impedance bandwidths is because activating one of the diodes creates shorted ring slot, and the position of the shortening PIN diode affects the current and field distributions, which in turn impacts both the total impedance bandwidth and the radiation pattern of the antenna.

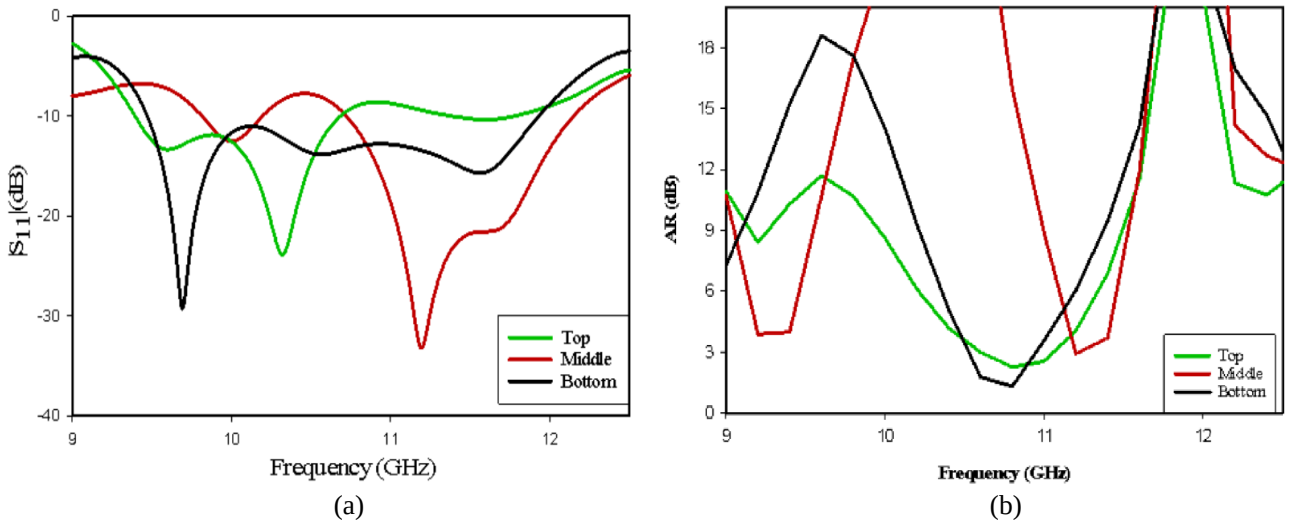

Figure 3. Simulated rectangular DRA for different switch positions (a) return losses, (b) axial ratio.

4. PROTOTYPING AND MEASUREMENTS

Figures 4(a) and (b) present the front and back views of the prototype of the rectangular DRA. The DRA has been bonded to the metallic ground plane using a double-sided adhesive copper tape with a thickness of 0.036 mm. In addition, the PIN diode has dimensions of 1.2 mm × 0.4 mm × 0.2 mm for length, width, and height. The diodes have been placed at the long sides of the feeding slot as illustrated

Table 1. Different switches positions when D1 is ON and D2 is OFF.

Switches Position	$\|S_{11}\|$%	AR BW%	Gain
Top	9.8%	3.8%	7.2 dBic
Middle	4.2%	null	6.5 dBi
Bottom	21.3%	3.9%	6.9 dBic

in Figure 2(b) and attached to the ground plane using conductive silver paint. Two biasing wires are connected to the two ground plane sections. The inner smaller section of the ground plane is biased through a plated hole, which passes through the substrate to create the required connection to the DC transmission line at the bottom of the substrate as shown in Figure 4(b). In addition, a groove has been etched at the lower DRA side with respective depth, length, and width of 0.5 mm, 8.6 mm, and 1.5 mm as shown in Figure 4(c). The purpose of this groove is to accommodate the height of PIN diodes so that the DRA can be positioned steadily on the ground plane without creating air gaps in between. The reflection coefficient, S_{11}, has been measured using a network analyser through a calibrated cable, and the radiation patterns have been measured using an anechoic chamber. As mentioned earlier, three polarisation states have been achieved from the proposed antenna as described in the following sections.

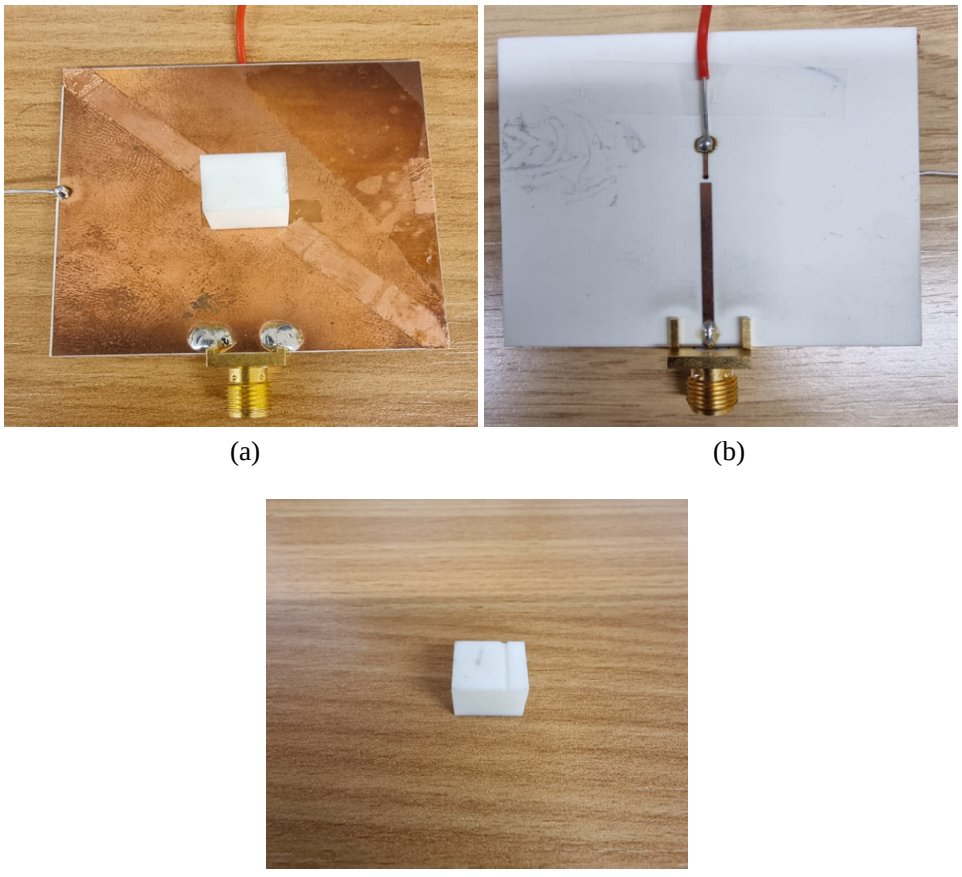

Figure 4. Prototype of the proposed antenna: (a) top view, (b) bottom view, (c) rectangular DRA with a groove.

4.1. Left-Hand Circular Polarization

In the first configuration, the first PIN diode, i.e., D1 in Figure 2(b), has been biased to be in the ON state while the other PIN diode, D2, is reverse biased. The positive DC signal is connected to the positive terminal, P, of D1 via the outer ground plane section, and the negative terminal is connected to the inner rectangular ground plane, which is connected to the common ground as mentioned earlier. The negative terminal, N, the terminal of D2 was connected to the positive DC to be in the OFF state. The reflection coefficient has been simulated and measured as illustrated in Figure 5 with a simulated impedance bandwidth of 21.6% that has been achieved over a frequency range of 9.6 to 11.9 GHz compared to a measured bandwidth of 21.4% due to the excitation of the TE_{113} higher-order mode at 10.6 GHz. Figure 6 presents the axial ratio and gain, where it can be observed that an AR bandwidth of 4% has been achieved with a maximum gain 6.9 dBic at 10.6 GHz as a result of exciting the aforementioned higher-order resonance mode. A close agreement has been achieved between simulated and measured data. In addition, the far field patterns are illustrated in Figure 7, where it is evident that a left-hand CP radiation has been achieved, since the left-hand CP electric field component, EL, is greater than the right-hand CP electric field component, ER, by 15 dBi at 10.6 GHz. Finally, the short magnetic and electric dipoles inside the rectangular DRA are depicted in Figures 8(a) and (b), where it is evident that the TE_{113} mode has been excited at 10.6 GHz.

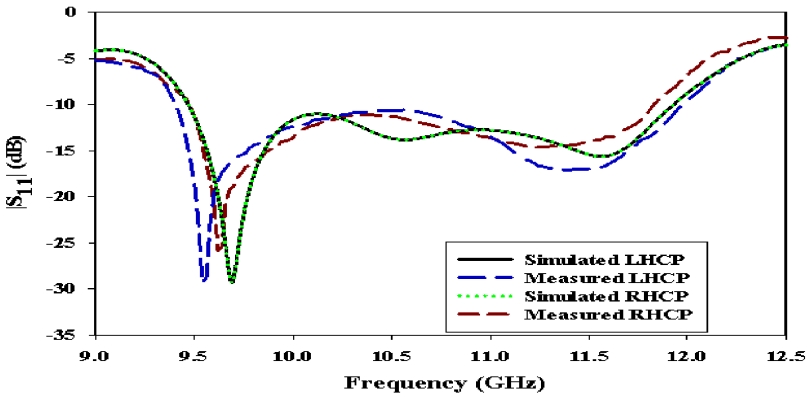

Figure 5. Simulated and measured return losses of DRA operating in the LHCP and RHCP states.

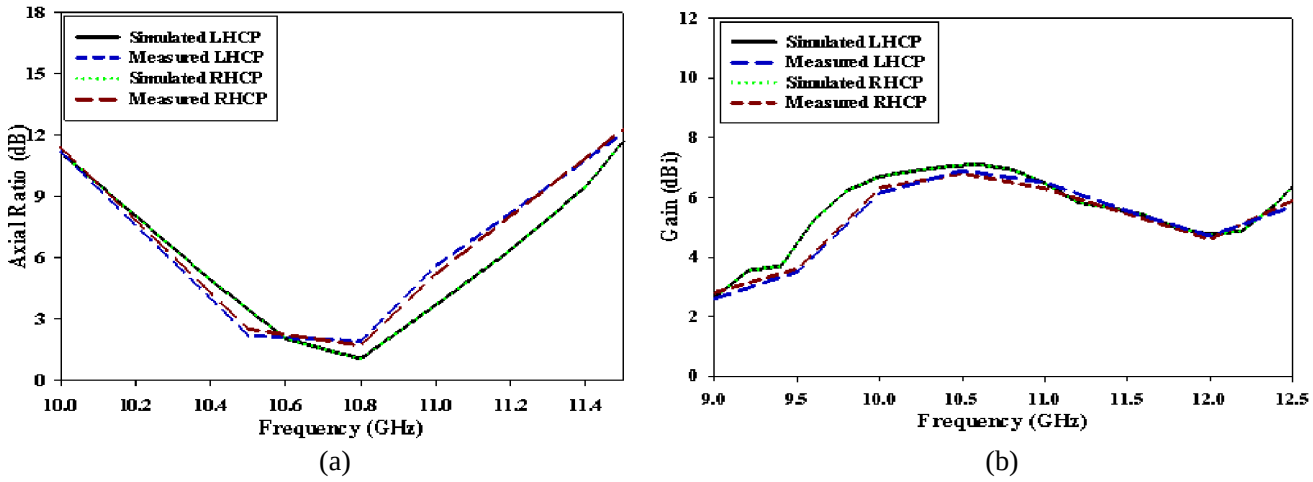

Figure 6. Simulated and measured rectangular DRA, (a) axial ratio, (b) gain.

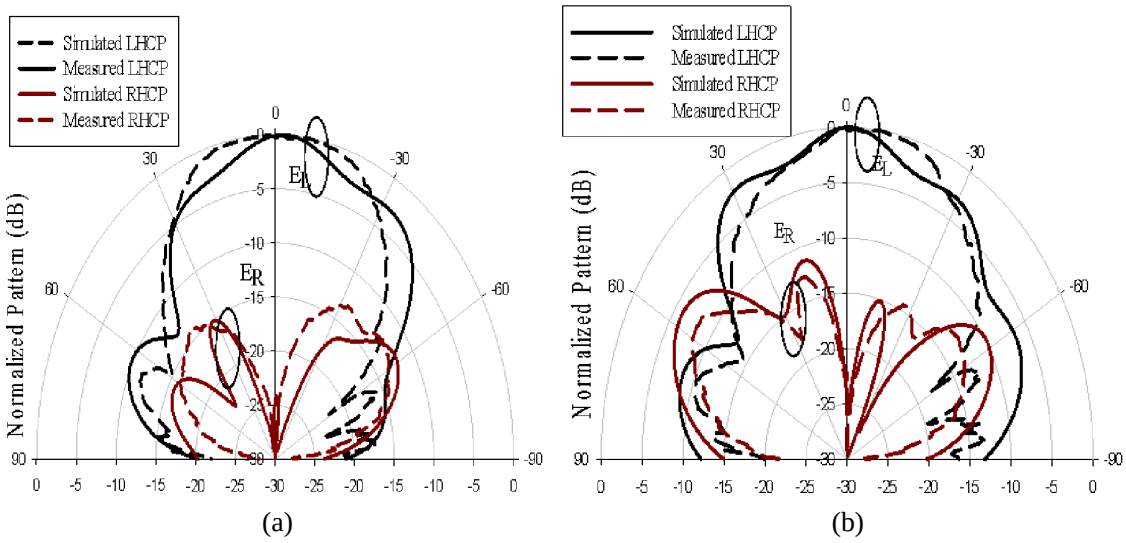

Figure 7. Simulated and measured normalized radiation patterns at 10.6 GHz, (a) E-plane, (b) H-plane.

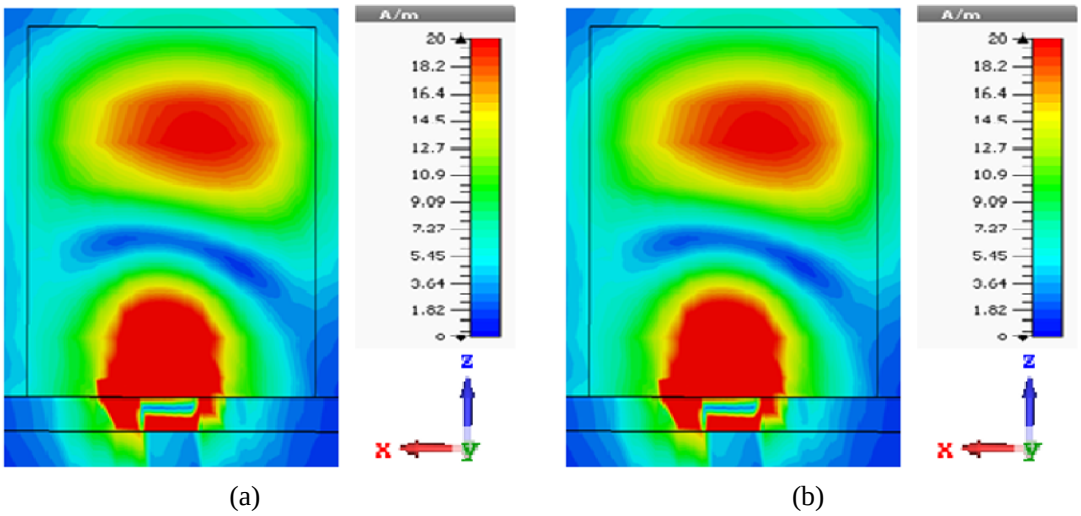

Figure 8. Rectangular DRA field distribution, (a) magnetic field, (b) electric field for the TE_{113} mode at 10.6 GHz.

4.2. Right-Hand Circular Polarization

In the second scenario, the PIN diode D1 has been switched to the OFF state, and D2 is switched to the ON state. As a result, the outer ground plane has been connected to the common ground, and the inner ground plane section is connected to the positive DC polarity. Therefore, the positive terminal of D2 is connected via the inner rectangular ground plane, and the negative terminal is connected to the outer ground plane. On the other hand, the positive terminal of D1 is connected to the outer ground plane, and the negative terminal is connected to the inner ground plane. Figure 5 illustrates the reflection coefficient with a close agreement between the simulated and measured impedance bandwidths of 21.3% and 21.1%, respectively. Once more, good agreement has been achieved between the measured and simulated data for the gain as well as axial ratio as illustrated in Figure 6. The achieved maximum gain is 6.9 dBic at 10.6 GHz with an AR bandwidth of 4%. Furthermore, the far field patterns are

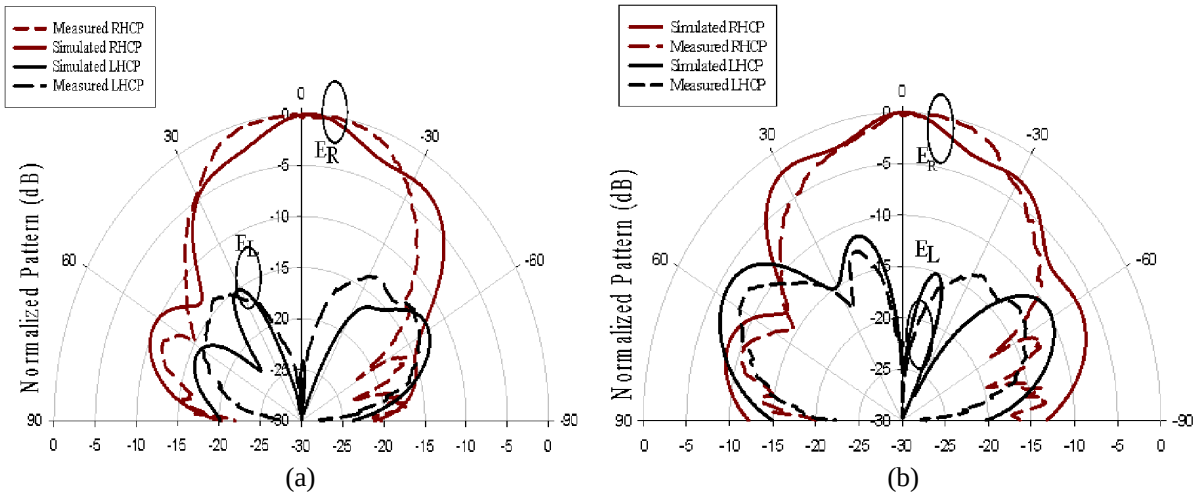

Figure 9. Simulated and measured normalized radiation patterns at 10.6 GHz, (a) E-plane, (b) H-plane.

presented in Figure 9, where it is evident that a right-hand CP radiation is achieved since the ER component is greater than the EL counterpart by 15 dBi at 10.6 GHz.

4.3. Linear Polarization

In the third scenario, both of the PIN diodes have not been biased, and hence they are switched to the OFF state. Figure 10(a) presents the reflection coefficient with an impedance bandwidth of 3.4% that extends from 10.2 to 10.5 GHz for the simulated and measured data. Figure 10(b) illustrates that the DRA offers a maximum gain of 6.5 dBi at 10.4 GHz with good agreement between simulated and measured data. The far-field patterns at 10.4 GHz are illustrated in Figure 11 with a reasonable agreement between measurements and simulations.

The examined antenna can be compared to other recently published works as shown below in Table 2.

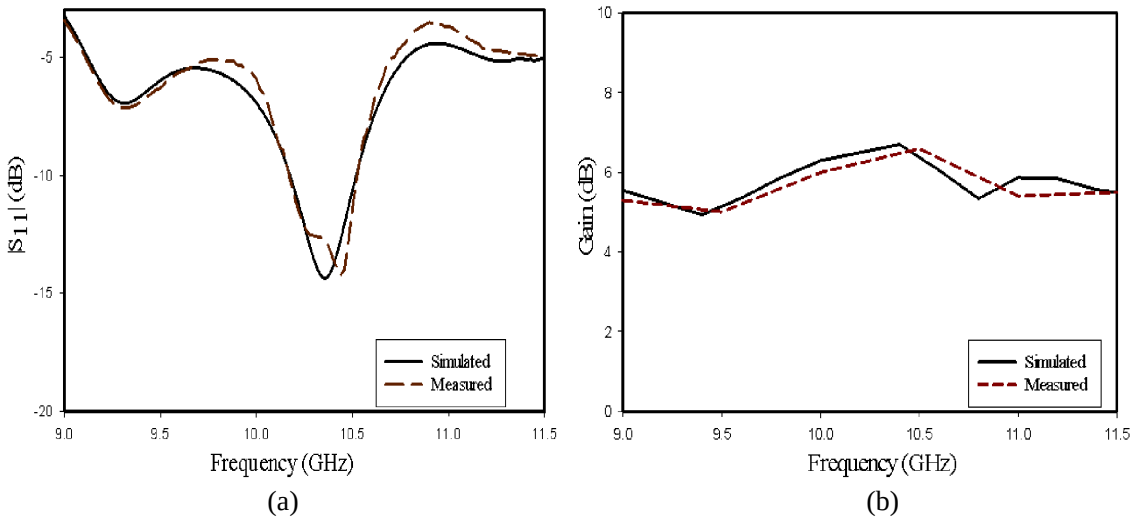

Figure 10. Linearly polarized rectangular DRA, (a) reflection coefficients, (b) gain.

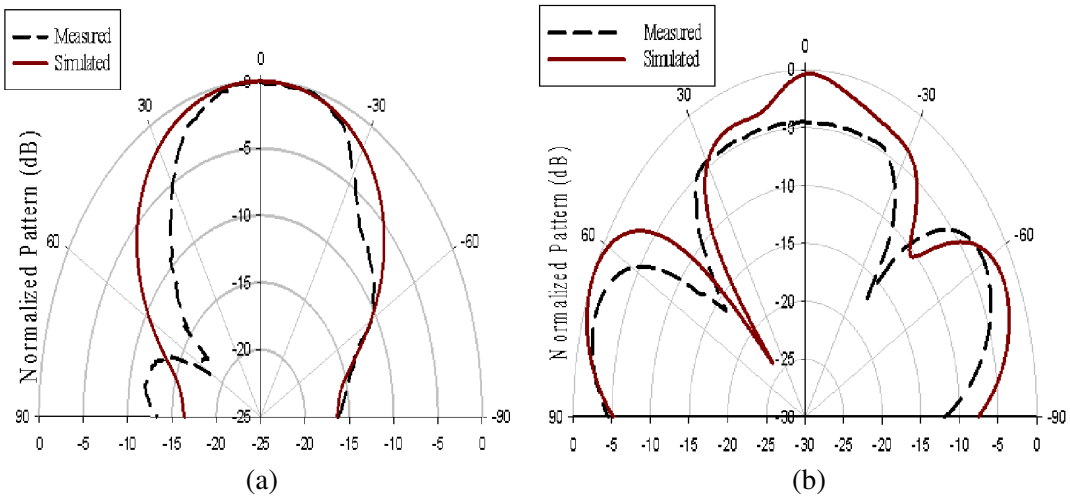

Figure 11. Simulated and measured normalized radiation patterns at 10.4 GHz, (a) E-plane, (b) H-plane.

Table 2. Comparison of currently published literature.

Ref.	Antenna Type	No. PIN diodes	Polarisation states	Gain	Antenna size
[11]	Cylindrical DRA	4	RHCP LHCP LP	5.5	$R = 0.25\lambda$, $h = 0.11\lambda$ Substrate $= 0.47\lambda \times 0.47\lambda \times 0.018\lambda$
[12]	Rectangular DRA	8	RHCP LHCP LP	4	$a = 0.13\lambda$, $b = 0.13\lambda$ and $h = 0.26\lambda$ Substrate = N/A.
[13]	Cylindrical DRA	2	RHCP LHCP LP	5.67	$R = 0.09\lambda$, $h = 0.17\lambda$ Substrate $= 0.66\lambda \times 0.66\lambda \times 0.017\lambda$
[14]	Patch	2	RHCP LHCP LP	4.6	$0.36\lambda \times 0.30\lambda \times 0.02\lambda$
[15]	Slot Array	4	RHCP LHCP	9.8	$2.3\lambda \times 2.3\lambda \times 0.017\lambda$
Proposed Antenna	Rectangular DRA	2	RHCP LHCP LP	6.9	$a = 0.36\lambda$, $b = 0.30\lambda$ and $h = 0.31\lambda$ Substrate $= 1.79\lambda \times 1.79\lambda \times 0.0\lambda$

5. CONCLUSIONS

This paper has examined a polarization reconfigurable rectangular DRA for applications in the X band. Controlling the two PIN diode switches enables the antenna to produce LP, LHCP, and RHCP radiations. The rectangular DRA proposed herein is easily constructed and has a simple structure. The results of the simulation show that the LHCP and RHCP radiations have reconfigurable polarization traits with a 21.3% impedance bandwidth ranging from 9.6 to 11.9 GHz. On the other hand, the LP state has a narrower impedance bandwidth of 3.4% ranging from 10.2 to 10.5 GHz. Furthermore, higher gain has reached approximately 6.9 dBic in all polarisations. The simulations and measurements agree well with each other. Benefits of the proposed antenna include a compact structure compared with other designs reported in the literature with a simple biasing mechanism, construction, and adjustment. It means that the antenna has the potential for numerous applications in wireless communication systems, particularly in relation to polarization diversity applications.

REFERENCES

1. Petosa, A. and A. Ittipiboon, "Dielectric resonator antennas: A historical review and the current state of the art," *IEEE Antennas and Propagation Magazine*, Vol. 52, No. 5, 91–116, 2010.
2. Solis, C., "Dielectric resonator antennas and bandwidth enhancement techniques," The University of Manchester, United Kingdom, 2015.
3. Ullah, U., M. F. Ain, and Z. A. Ahmad, "A review of wideband circularly polarized dielectric resonator antennas," *China Communications*, Vol. 14, No. 6, 65–79, 2017.
4. Esmaeili, M. and J.-J. Laurin, "Polarization reconfigurable slot-fed cylindrical dielectric resonator antenna," *Progress In Electromagnetics Research*, Vol. 168, 61–71, 2020.
5. Costantine, J., Y. Tawk, S. E. Barbin, and C. G. Christodoulou, "Reconfigurable antennas: Design and applications," *Proceedings of the IEEE*, Vol. 103, No. 3, 424–437, 2015.
6. Monti, G., R. De Paolis, and L. Tarricone, "Design of a 3-state reconfigurable CRLH transmission line based on MEMS switches," *Progress In Electromagnetics Research*, Vol. 95, 283–297, 2009.
7. Varlamos, P. and C. N. Capsalis, "Electronic beam steering using switched parasitic smart antenna arrays," *Progress In Electromagnetics Research*, Vol. 36, 101–119, 2002.
8. Weedon, W. H., W. J. Payne, and G. M. Rebeiz, "MEMS-switched reconfigurable antennas," *IEEE Antennas and Propagation Society International Symposium. 2001 Digest. Held in conjunction with: USNC/URSI National Radio Science Meeting (Cat. No. 01CH37229)*, Vol. 3, 654–657, IEEE, 2001.
9. Chen, Z. and H. Wong, "Liquid dielectric resonator antenna with circular polarization reconfigurability," *IEEE Transactions on Antennas and Propagation*, Vol. 66, No. 1, 444–449, 2017.
10. Wang, M. and Q.-X. Chu, "A wideband polarization-reconfigurable water dielectric resonator antenna," *IEEE Antennas and Wireless Propagation Letters*, Vol. 18, No. 2, 402–406, 2019.
11. Iqbal, A., M. I. Waly, A. Smida, and N. K. Mallat, "Dielectric resonator antenna with reconfigurable polarization states," *IET Microwaves, Antennas & Propagation*, Vol. 15, No. 7, 683–690, 2021.
12. Dhar, S., K. Patra, R. Ghatak, B. Gupta, and D. R. Poddar, "Reconfigurable dielectric resonator antenna with multiple polarisation states," *IET Microwaves, Antennas & Propagation*, Vol. 12, No. 6, 895–902, 2017.
13. Zhong, L., "A polarization reconfigurable cylindrical dielectric resonator antenna," *Progress In Electromagnetics Research M*, Vol. 93, 1–9, 2020.
14. Fakharian, M., P. Rezaei, and A. Orouji, "Reconfigurable multiband extended U-slot antenna with switchable polarization for wireless applications," *IEEE Antennas and Propagation Magazine*, Vol. 57, No. 2, 194–202, 2015.
15. Mousavi, Z., P. Rezaei, and V. Rafii, "Single layer CPSSA array with change polarization diversity in broadband application," *International Journal of RF and Microwave Computer-Aided Engineering*, No. 4, e21075, 2017.
16. MACOM, "https://www.macom.com/products/product-detail/MA4SPS402," 2022.
17. Petosa, A. and S. Thirakoune, "Rectangular dielectric resonator antennas with enhanced gain," *IEEE Transactions on Antennas and Propagation*, Vol. 59, No. 4, 1385–1389, 2011.